arXiv:cond-mat/0311291v1 [cond-mat.str-el] 12 Nov 2003

Density-matrix renormalisation group approach to quantum impurity problems

S Nishimoto†and E Jeckelmann‡

†Fachbereich Physik, Philipps-Universität, 35032 Marburg, Germany
‡Institut für Physik, KOMET 337, Johannes Gutenberg-Universität, 55099 Mainz, Germany

E-mail: Eric.Jeckelmann@Uni-Mainz.DE

Abstract. A dynamic density-matrix renormalisation group approach to the spectral properties of quantum impurity problems is presented. The method is demonstrated on the spectral density of the flat-band symmetric single-impurity Anderson model. We show that this approach provides the impurity spectral density for all frequencies and coupling strengths. In particular, Hubbard satellites at high energy can be obtained with a good resolution. The main difficulties are the necessary discretisation of the host band hybridised with the impurity and the resolution of sharp spectral features such as the Abrikosov-Suhl resonance.

PACS numbers: 71.27.+a,71.55.Ak,72.15.Qm,78.67.Hc,05.10.Cc

Submitted to: *J. Phys.: Condens. Matter*

1. Introduction

The single-impurity Anderson model (SIAM) was invented more than forty years ago to describe dilute magnetic impurities in metals [1]. In recent years it has become a generic model for the physics of strong local electron interactions [2] and is currently attracting much interest as a model for studying quantum dots coupled to leads [3]. Its importance has also grown with the advent of the dynamical mean-field theory (DMFT) [4]. Within the DMFT approach a lattice model such as the Hubbard model in the limit of high dimensions is mapped onto an effective SIAM which is determined self-consistently. Although the properties of the SIAM are generally well understood from numerous studies based on various methods, the situation is not fully satisfactory as far as the dynamic properties are concerned, especially the zero-temperature high-frequency dynamics. Many-body theories, such as perturbation theory or the local moment approach (LMA) [5, 6], provide an explanative (and often accurate) picture of quantum impurity dynamics but their accuracy is not known *a priori*. Quantum Monte Carlo (QMC) simulations combined with the Maximum Entropy Method [7] give accurate results at finite temperature but extrapolations of the dynamic properties to low-temperature are more difficult. The Numerical Renormalisation Group (NRG) [8, 9, 10] allows one to determine the low-energy dynamics of quantum impurity models almost exactly but this method is less precise at high-energy because of the necessary logarithmic discretisation of the host band.

The NRG has been applied to various quantum impurity problems with great success but it has proven more difficult to apply NRG transformations to quantum lattice models. These difficulties provided the motivation for the development of the density-matrix renormalisation group (DMRG) a decade ago [11]. DMRG is one of the most powerful numerical techniques for studying quantum lattice many-body systems [12]. Recently a dynamical DMRG (DDMRG) method has been developed to calculate dynamic correlation functions at zero temperature in quantum lattice models [13, 14]. Here we extend this approach to the calculation of the spectral properties in quantum impurity models. The method is demonstrated on the flat-band symmetric SIAM. We show that DDMRG can provide the spectral density of the SIAM for all frequencies and coupling strengths. In particular, the high-energy spectrum can be determined with a good resolution. Thus the DDMRG approach is a very useful complement to existing techniques for calculating the dynamics of quantum impurity models.

The Hamiltonian of the SIAM is

$$\hat{H} = \sum_{k\sigma} \epsilon_k \hat{f}^\dagger_{k\sigma} \hat{f}_{k\sigma} + U \left(\hat{n}_{d\uparrow} - \frac{1}{2} \right) \left(\hat{n}_{d\downarrow} - \frac{1}{2} \right) + \sum_{k\sigma} V_k \left(\hat{f}^\dagger_{k\sigma} \hat{d}_\sigma + \hat{d}^\dagger_\sigma \hat{f}_{k\sigma} \right), \tag{1}$$

where $\hat{d}^\dagger_\sigma$ ($\hat{d}_\sigma$) creates (annihilates) an electron with spin $\sigma =\uparrow, \downarrow$ in a local level (the impurity site), $\hat{n}_{d\sigma} = \hat{d}^\dagger_\sigma \hat{d}_\sigma$ and $\hat{f}^\dagger_\sigma$ ($\hat{f}_\sigma$) creates (annihilates) an electron with spin σ in an eigenstate of the (non-interacting) host band with dispersion ϵ_k. The sum over the index k runs over all states of the host band. The hybridisation between the local impurity state and the delocalised band state k is given by the positive couplings V_k.

Electrons in the local level are subject to a Coulomb repulsion U. (The impurity site potential is set by $\mu = -U/2$ as we will discuss the symmetric SIAM only.)

The impurity one-particle Green's function can be written ($\eta \to 0^+$)

$$G_\sigma(\omega) = \left\langle \hat{d}_\sigma^\dagger \frac{1}{\hat{H} - E_0 + \omega - i\eta} \hat{d}_\sigma \right\rangle + \left\langle \hat{d}_\sigma \frac{1}{E_0 - \hat{H} + \omega + i\eta} \hat{d}_\sigma^\dagger \right\rangle, \tag{2}$$

where E_0 is the ground state energy and $\langle \ldots \rangle$ represents a ground state expectation value. In most studies of quantum impurity problems an objective is the computation of the impurity spectral density

$$D_\sigma(\omega) = -\frac{1}{\pi} \mathrm{sgn}(\omega) \mathrm{Im} G_\sigma(\omega) = A_\sigma(\omega) + B_\sigma(\omega) \tag{3}$$

with

$$A_\sigma(\omega \leq 0) = \lim_{\eta \to 0} \left\langle \hat{d}_\sigma^\dagger \frac{\eta}{\pi[(\hat{H} - E_0 + \omega)^2 + \eta^2]} \hat{d}_\sigma \right\rangle \tag{4}$$

$$B_\sigma(\omega \geq 0) = \lim_{\eta \to 0} \left\langle \hat{d}_\sigma \frac{\eta}{\pi[(\hat{H} - E_0 - \omega)^2 + \eta^2]} \hat{d}_\sigma^\dagger \right\rangle \tag{5}$$

and $A_\sigma(\omega \geq 0) = B_\sigma(\omega \leq 0) = 0$. The spectral density fulfills the sum rule

$$\int_{-\infty}^{\infty} D(\omega) \mathrm{d}\omega = 1. \tag{6}$$

The impurity spectral density of the SIAM model depends on the parameter U and the hybridisation function

$$\Delta(\omega) = \pi \sum_k |V_k|^2 \delta(\omega - \epsilon_k) \geq 0 \, . \tag{7}$$

For a symmetric hybridisation function $\Delta(\omega) = \Delta(-\omega)$ the SIAM has a particle-hole symmetry. As consequences, the Green's function (2) is an odd function of ω but the spectral density (3) is an even function, $D_\sigma(\omega) = D_\sigma(-\omega)$ [or $A_\sigma(\omega) = B_\sigma(-\omega)$], and the Fermi energy remains pinned at $\omega = 0$ for all U. Furthermore, as the total spin is conserved in the SIAM, $G_\sigma(\omega) = G_{-\sigma}(\omega)$.

In the rest of this paper we will explain how the spectral density of a quantum impurity problem such as the symmetric SIAM can be calculated with DDMRG. To illustrate the various approaches that we have tested we show results for a well-known particular case of the SIAM: the flat-band model [2]. In that case, the host band width is taken to be much larger than any other energy scales and the hybridisation function is assumed to be constant on these scales, $\Delta(\omega) = \Delta_0$. Our goal is then to compute $D_\sigma(\omega)$ in the relevant energy window $-W/2 < \omega < W/2$ with $W/2 > U/2, \Delta_0$. It should be noted that a Friedel sum rule

$$D_\sigma(\omega = 0) = \frac{1}{\pi \Delta_0} \tag{8}$$

holds at the Fermi energy $\omega = 0$ for all $U \geq 0$ in the flat-band symmetric SIAM. In all numerical results presented here the energy scale is set by $\Delta_0 = 1$.

2. DMRG method for quantum impurity problems

Since the invention of DMRG there have been numerous applications of this method to systems made of one or more impurities coupled to (generally interacting) one-dimensional hosts [15]. Recently the growing interest for quantum impurity problems has spurred the development of DMRG techniques for investigating the more relevant problems of impurities coupled to arbitrary non-interacting host bands both in the context of quantum dots [16] and of DMFT calculations [17, 18].

A direct application of the usual DMRG algorithms to the SIAM Hamiltonian (1) is possible but extremely inefficient because it includes "long-range" hopping terms (more precisely, an electron can go from one site to any other site in just two hops). A better approach is the transformation of the Hamiltonian (1) into a linear chain with nearest-neighbor interactions only (as in a NRG calculation [8])

$$\begin{aligned}\hat{H} = V \sum_{\sigma} \left(\hat{c}^{\dagger}_{1\sigma} \hat{d}_{\sigma} + \hat{d}^{\dagger}_{\sigma} \hat{c}_{1\sigma} \right) + U \left(\hat{n}_{d\uparrow} - \frac{1}{2} \right) \left(\hat{n}_{d\downarrow} - \frac{1}{2} \right) \\ + \sum_{j\sigma} a_j \hat{c}^{\dagger}_{j\sigma} \hat{c}_{j\sigma} + \sum_{j\sigma} \lambda_j \left(\hat{c}^{\dagger}_{j\sigma} \hat{c}_{j+1\sigma} + \hat{c}^{\dagger}_{j+1\sigma} \hat{c}_{j\sigma} \right). \end{aligned} \tag{9}$$

The new fermion operators $\hat{c}_{j\sigma}$ corresponds to electronic states in the host band and are related to the original representation by a canonical transformation

$$\hat{c}_{j\sigma} = \sum_{k} M_{jk} \hat{f}_{k\sigma}. \tag{10}$$

The orthogonal matrix M_{jk}, the diagonal terms a_j and the nearest-neighbor hopping terms λ_j are calculated with the Lanczos iterative algorithm for tridiagonalising a symmetric matrix starting from the initial vector $\{M_{1,k} = V_k/V\}$ with $V^2 = \sum_k V_k^2$. This calculation must be carried out with very high numerical accuracy (quadruple or higher precision for floating-point operations) but does not present any other difficulty. If the original Hamiltonian (1) is particle-hole symmetric, the diagonal terms a_j vanish.

The Hamiltonian (9) describes an impurity coupled to one end of a one-dimensional chain representing the host band states (see figure 1). Here we will use only this configuration. However, one can easily imagine different configurations such as an impurity site located between two chains as also shown in figure 1. In that case, the left and right chains could correspond to band states below ($\epsilon_k < 0$) and above ($\epsilon_k > 0$) the Fermi energy, respectively. Another possibility is that the left and right chains could correspond to up-spin and down-spin band states, respectively. The transformation (10) described above can easily be adapted for either cases. It can also be generalised to more complicated impurity problems with more than one local level or more than one host band.

The finite-system DMRG algorithm [11, 12] can be used to calculate ground state properties of the Hamiltonian (9). In particular, the ground state wavefunction $|\Psi_0\rangle$ and the ground state energy E_0 can readily be obtained. To compute dynamic properties such as the impurity Green's function (2) we use the dynamical DMRG [14]. This

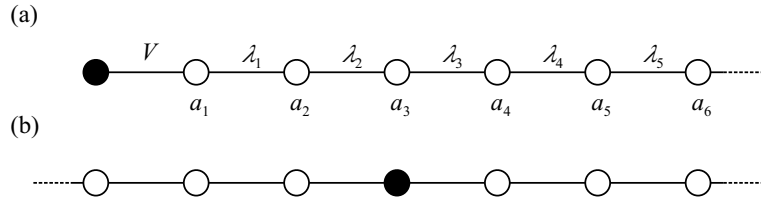

Figure 1. One-dimensional lattice configurations for applying a DMRG algorithm to quantum impurity problems: (a) Impurity site (solid circle) at one end of the chain representing the host band (open circles). (b) Impurity site in the middle of two chains.

approach is based on a variational principle. One can easily show that for $\eta > 0$ and a fixed frequency ω the minimum of the functional

$$W(\Psi) = \left\langle \Psi \left| \left(E_0 + \omega - \hat{H}\right)^2 + \eta^2 \right| \Psi \right\rangle + \eta \left\langle \Psi_0 \left| \hat{d}_\sigma \right| \Psi \right\rangle + \eta \left\langle \Psi \left| \hat{d}_\sigma^\dagger \right| \Psi_0 \right\rangle \tag{11}$$

with respect to all quantum states $|\Psi\rangle$ is

$$W(\Psi_{\min}) = \left\langle \Psi_0 \left| \hat{d}_\sigma \frac{-\eta^2}{\left(E_0 + \omega - \hat{H}\right)^2 + \eta^2} \hat{d}_\sigma^\dagger \right| \Psi_0 \right\rangle . \tag{12}$$

The functional minimum is related to the convolution of the spectral density (5) with a Lorentz distribution of width η by

$$W(\Psi_{\min}) = -\pi\eta B_\sigma^\eta(\omega). \tag{13}$$

A similar result is obtained for the spectral density (4) if one substitutes $\hat{d}_\sigma$ for $\hat{d}_\sigma^\dagger$, $-\omega$ for ω and $A_\sigma^\eta(\omega)$ for $B_\sigma^\eta(\omega)$ in the above equations.

The DDMRG method consists essentially in minimising the functional (11) numerically using the finite-system DMRG algorithm. Thus DDMRG provides the spectral densities $A_\sigma^\eta(\omega)$ and $B_\sigma^\eta(\omega)$ for a finite broadening η. The full spectral density (3) convolved with the Lorentz distribution

$$D_\sigma^\eta(\omega) = \int_{-\infty}^{\infty} \mathrm{d}\omega' D_\sigma(\omega') \frac{\eta}{\pi[(\omega - \omega')^2 + \eta^2]} \tag{14}$$

is given by the sum of $A_\sigma^\eta(\omega)$ and $B_\sigma^\eta(\omega)$. The real part of the Green's function can be calculated with no additional computational cost but is generally less accurate. The necessary broadening of spectral functions in DDMRG calculations is actually very useful for studying continuous spectra or doing a finite-size scaling analysis [14].

The objective of our DMRG simulations is to obtain physical quantities with a sufficient accuracy at the lowest possible computational cost. For this purpose, the lattice configuration used in the present work makes necessary an adaptation of the usual DMRG principles for measurements. In standard DMRG calculations the one-dimensional lattice is split in two blocks of sites separated by two intermediate sites [11, 12]. Calculations are carried out in an effective Hilbert space of dimension $D \approx n^2 m_L m_R$, where n is the number of states per site ($n = 4$ counting the spin degeneracy in our case) and $m_{L,R}$ are the numbers of states used to describe the left and

right blocks, respectively. Note that $m_{L,R} \approx \min(m, 4^{N_{L,R}})$, where m is the maximum number of density-matrix eigenstates kept and N_L and N_R are the numbers of sites in the left and right blocks, respectively. The DMRG method errors diminish (often exponentially fast) as m is increased while the computational cost increases as m^3 (at least in theory). During a DMRG simulation the position where the chain is split is moved repeatedly through all sites and the measurement precision for a fixed number m varies with that position. Measurements of local quantities such as the density $\hat{c}^\dagger_{j\sigma}\hat{c}_{j\sigma}$ are most accurate if the site j is one of the two intermediate sites. Measurements of global quantities, such as the ground state energy or long-range correlations, are most accurate if the chain is split in two blocks of equal size because the effective Hilbert space dimension D is maximal then. In the present application we have found that it is necessary to compromise in order to optimize the ratio between accuracy and computational cost in calculations of the spectral density for an impurity located at a chain end. Measurements have to be done as close as possible to the impurity but far enough from the chain end for the effective Hilbert space to approach its maximal dimension $D = n^2m^2$. This implies that measurements are to be done when the left block has reached the size of $N_L \approx \ln(m)/\ln(4)$ sites (assuming the impurity to be at the left chain end).

In practice, we keep enough density-matrix eigenstates to make (D)DMRG truncation errors negligible (we have used up to $m = 800$ states in the present work). Thus our DDMRG results for finite systems are numerically exact in the same sense as "exact diagonalisation" results are. The main source of errors are finite-size effects, which corresponds to the discretisation of the continuous host band in the SIAM and are discussed in the next section.

In figure 2 we show the spectral density of the flat-band symmetric SIAM calculated with DDMRG for $U = 0$. The exact spectral density is a Lorentzian of width Δ_0. With the broadening (14) it becomes

$$D^\eta_\sigma(\omega) = \frac{\Delta_0 + \eta}{\pi[\omega^2 + (\Delta_0 + \eta)^2]}. \tag{15}$$

On the scale of figure 2 there is no visible difference between our numerical results and this exact result, which demonstrates the accuracy of our method. Note that the $U = 0$ limit is a relevant accuracy test. The hybridisation $\Delta(\omega)$ with the host band is renormalised in the density-matrix renormalisation and thus our method could become exceptionally accurate for some specific hybridisations [for instance, $\Delta(\omega) = 0$] but the local Coulomb interaction U is always treated exactly and thus does not affect the method accuracy directly.

With DDMRG the computational cost (memory and processor time) of computing $D^\eta_\sigma(\omega)$ for a single frequency ω is proportional to the number N of sites in the system. In practice, the total processor time for calculating the full spectrum grows as $\sim N^3$ because one usually reduces η and increases the frequency resolution as N is increased.

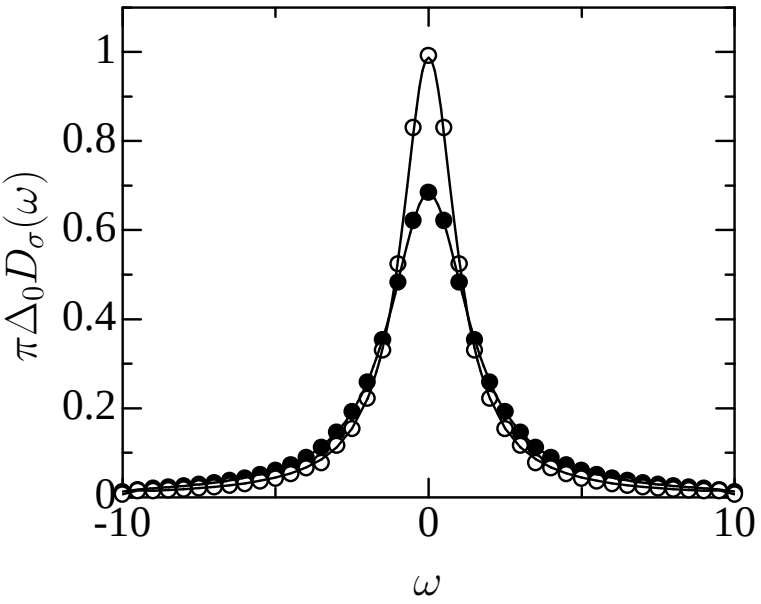

Figure 2. Spectral density at $U = 0$ calculated with a constant host band discretisation (solid circles) for $W = 20\Delta_0, N = 59, \Delta\epsilon \approx 0.34\Delta_0$, and $\eta = 0.5$, then deconvolved (open circles). Solid lines show the exact results (15) without broadening and with $\eta = 0.5$ for comparison.

3. Discretisation of the host band

We are interested in the properties of the SIAM with a continuous host band and a continuous hybridisation function $\Delta(\omega)$ but DMRG calculations can be performed on finite lattices only. Therefore, we must discretise the host band and carry out DMRG calculations for a finite number N of host band eigenstates corresponding to energies $\epsilon_k (k = 1, \ldots, N)$, then extrapolate the results to a continuous host band ($N \to \infty$). Choosing an appropriate discretisation of the host band (i.e., selecting the N band state energies ϵ_k) turns out to be the greatest difficulty in applying DDMRG to the SIAM.

The spectral density (4) [or similarly (5)] can be written in the Lehmann representation

$$A_\sigma(\omega) = \sum_n \left| \left\langle \Psi_n \left| \hat{d}_\sigma \right| \Psi_0 \right\rangle \right|^2 \delta(\omega + E_n - E_0), \tag{16}$$

where $|\Psi_n\rangle$, $n = 0, 1, \ldots$, design the eigenstates of $\hat{H}$ contributing to $A_\sigma(\omega)$ (i.e., with non-vanishing matrix elements) and E_n their respective energies. On a finite lattice this spectrum is always discrete. To determine the exact SIAM spectral density for $N \to \infty$ it is necessary to use a broadening η larger than the space $E_{n+1} - E_n$ between two consecutive eigenstates in dense parts of the spectrum (for instance, in continuous parts of the spectrum) [14]. In the flat-band SIAM (and also in self-consistent SIAM derived in DMFT calculations for the Hubbard model [17]) the distribution of excited states contributing to the spectral density for finite N is essentially determined by the

distribution of selected energies ϵ_k. Therefore, we must use

$$\eta > E_{n+1} - E_n \sim \epsilon_{k+1} - \epsilon_k. \tag{17}$$

In other words, the host band discretisation directly limits the resolution of spectral density calculations. Note that this is a general difficulty for all methods based on a discretisation of the SIAM, not only for DDMRG calculations. For instance, a similar problem limits the resolution of NRG calculations at high energy.

In practice, we choose N values ϵ_k in the relevant energy window $|\omega| < W/2$ and calculate the corresponding hybridisation terms

$$V_k^2 = \frac{1}{\pi} \int_{\delta_k}^{\delta_{k+1}} \Delta(\omega) \mathrm{d}\omega, \tag{18}$$

where $\delta_k = (\epsilon_{k-1} + \epsilon_k)/2$. If $\Delta(\omega)$ varies slowly for $\omega \approx \epsilon_k$ on the scale $\Delta\epsilon_k = (\epsilon_{k+1} - \epsilon_{k-1})/2$ then $V_k^2 \approx \Delta(\omega = \epsilon_k)\Delta\epsilon_k/\pi$. For the flat-band SIAM that we are considering here this last equation is obviously exact. To preserve the particle-hole symmetry in the discrete SIAM we only include pairs of band states with opposite energies in the N selected values. For even N this means that there are $N/2$ different pairs $(\epsilon_k, -\epsilon_k)$, while for odd N there are $(N-1)/2$ such pairs and a state at $\epsilon_k = 0$. Including the impurity site, the total number of sites in the lattice is thus $N+1$. The ground state contains an equal number of electrons and has a minimal total spin $S = 0$ for odd N and $S = 1/2$ for even N. Note that in that last case ($S \neq 0$) we need to compute the spectral density for both $\sigma =\uparrow$ and $\sigma =\downarrow$ and take the average, as the spin-flip symmetry $\sigma \leftrightarrow -\sigma$ is broken. It is thus more efficient to work with an odd number N of host band states.

The simplest discretisation scheme consists in choosing N equidistant energies ϵ_k ($\Delta\epsilon_k = \Delta\epsilon \approx W/N$) in the relevant energy window ($W/2 > |\epsilon_k|$). In that case we use a constant broadening $\eta \approx \Delta\epsilon$. This approach has been used for the $U = 0$ results shown in figure 2. A constant discretisation is sufficient provided that the spectrum does not contain any structure with a width smaller than $\Delta\epsilon \propto 1/N$, which is readily achieved in the weak-coupling SIAM. It is well-known [2, 5, 10] that for intermediate to strong couplings U the broad spectral feature around $\omega = 0$ shrinks to a sharp peak (the so-called Abrikosov-Suhl resonance). The spectral weight is progressively transfered to two Hubbard satellites around $\omega \approx \pm U/2$ for increasing U. For instance, in figure 3 we show the spectral density for the intermediate coupling $U = 2.5\pi\Delta_0$ calculated with a constant discretisation $\Delta\epsilon \approx 0.34\Delta_0$ and a broadening $\eta = 0.5\Delta_0$. This spectrum agrees qualitatively with LMA and NRG results [5, 10]. Quantitatively, however, the DDMRG spectrum is obviously inaccurate, especially around $\omega \approx 0$. For instance, at the Fermi level the Friedel sum rule (8) is clearly not fulfilled. As for the $U = 0$ case this apparent discrepancy is due to the broadening η.

To obtain better results one can perform calculations with a higher resolution (which means smaller $\eta \approx \Delta\epsilon \sim 1/N$ and thus larger lattice size N) and possibly extrapolate to the limits $\eta \to 0$ and $N \to \infty$. In figure 4 we show $D_\sigma^\eta(\omega = 0)$ calculated with DDMRG at $U = 2.5\pi\Delta_0$ for several values of η. For comparison we also show the

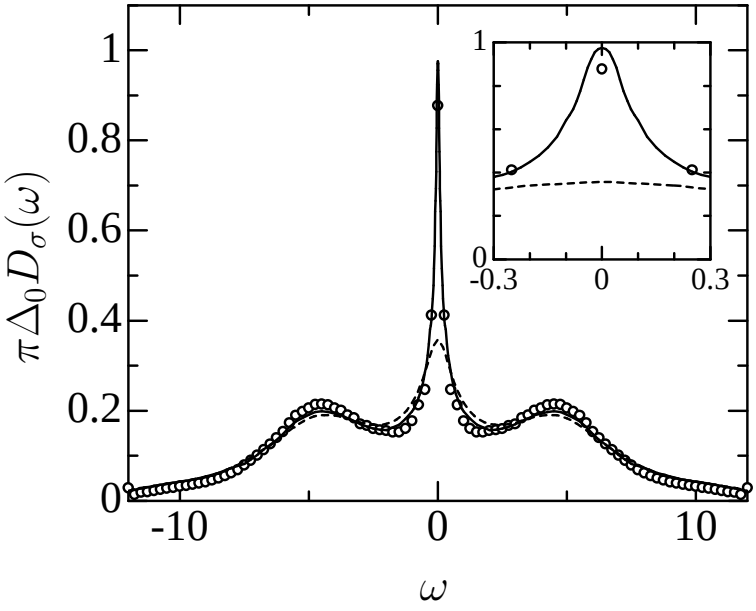

Figure 3. Spectral density for $U = 2.5\pi\Delta_0$ and $W = 24\Delta_0$. Calculated for a constant discretisation $\Delta\epsilon \approx 0.34\Delta_0$ and $\eta = 0.5\Delta_0$ (dashed line), calculated using variable discretisation $0.2 \geq \Delta\epsilon/\Delta_0 \geq 0.0059$ and broadening $0.25 \geq \eta/\Delta_0 \geq 0.01$ (solid line), and calculated using a variable discretisation $0.76 \geq \Delta\epsilon/\Delta_0 \geq 0.16$ and a constant broadening $\eta = 0.25\Delta_0$ then deconvolved (circles). Inset: expanded view around the Fermi level $\omega = 0$.

exact scaling for the non-interacting ($U = 0$) case. Clearly, $D_\sigma^\eta(\omega = 0)$ tends to the exact result as $\eta \to 0$ but the convergence is slow and will become worse for sharper resonances (larger U). For instance, for $U = 8\pi\Delta_0$ we can already clearly observe a very sharp Abrikosov-Suhl resonance using a resolution of $\Delta\epsilon \approx \eta = 10^{-4}\Delta_0$ but the height of the peak is only $D_\sigma^\eta(\omega = 0) \approx 0.06/\pi\Delta_0$. Actually, one can guess that a broadening η smaller than the Kondo scale $\propto \exp(-\pi U/8\Delta_0)$ [2, 5] is required to obtain the low-energy spectral density with a good resolution and accuracy. Therefore, the required system size $N \sim \eta^{-1} \propto \exp(\pi U/8\Delta_0)$ increases exponentially with U if one uses a constant discretisation. This approach is clearly not practicable.

As an interest of many quantum impurity problems is the investigation of sharp resonances in the spectral density and a analogous sharp quasi-particle peak is an essential feature of DMFT calculations, it is desirable to achieve a high accuracy and resolution for these spectral features too. A better approach is the use of a variable discretisation. For instance, one can select two sets of equidistant energies ϵ_k in the host band with a energy resolution $\Delta\epsilon$ for high energies $W/2 > |\epsilon_k| > W^*/2$ and with another energy resolution $\Delta\epsilon' < \Delta\epsilon$ for $|\epsilon_k| < W^*/2$ (see figure 5). In that case the broadening η also depends on ω. Typically, we use $\eta \approx \Delta\epsilon$ for $W/2 > |\omega| > W^*/2$ and $\eta \approx \Delta\epsilon'$ for $|\omega| < W^*/2$. This allows us to obtain the spectral density around the Abrikosov-Suhl resonance with a much higher resolution for a given number of host band sites N. It is also possible to use more than two different energy resolutions, to

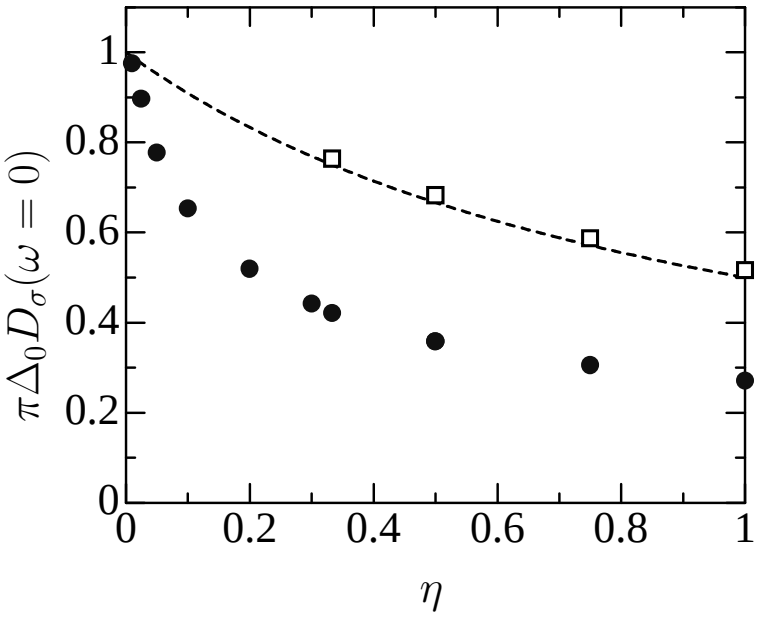

Figure 4. Fermi level spectral density $\pi\Delta_0 D_\sigma^\eta(\omega=0)$ as a function of the broadening η. Exact result for $U=0$ (dashed line) and DDMRG results for $U=0$ (squares) and $U=2.5\pi\Delta_0$ (circles).

use a higher energy resolution for the high energy sector than for the low energy sector, or even to select a higher resolution at intermediate energies (see figure 5). Moreover, it is possible to combine the results of the high-resolution sectors obtained with different variable discretisations in a single high resolution spectrum.

This approach allows us to achieve a resolution which is significantly better than with the constant discretisation for the same number of host band states N. For instance, figure 3 shows the spectral density obtained with variable discretisation $\Delta\epsilon$ and broadening η ranging from $\Delta\epsilon = 0.2\Delta_0$ ($\eta = 0.25\Delta_0$) for the Hubbard satellites to $\Delta\epsilon = 0.0059\Delta_0$ ($\eta = 0.01\Delta_0$) for $\omega \to 0$. This approach clearly gives much better results for the sharp Abrikosov-Suhl resonance than the constant discretisation approach. The Friedel sum rule (8) at the Fermi level is fulfilled within 3 %. It should be noted that this approach is not without problem. The most obvious drawback is that a variable broadening $\eta = \eta(\omega)$ breaks the sum rule (6) and can significantly change the spectrum shape if it varies faster than the bare spectrum as a function of ω. (This could be the case for the Abrikosov-Suhl resonance shown as a solid line in the inset of figure 3.)

To take advantage of the higher resolution provided by a variable discretisation while keeping the benefit of a constant broadening η we have devise the following scheme. The relevant energy window is split into several intervals. For each interval, a DDMRG calculation is done using a variable discretisation with a high resolution in that interval and a lower resolution outside. The spectral function is calculated for frequencies in that interval. Then the results obtained in each calculation are combined into a full spectrum. The computational effort is equal to that of a single calculation with a

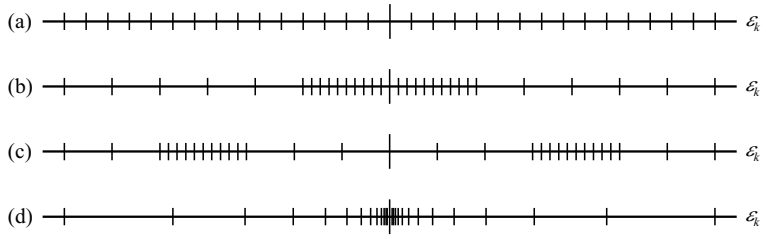

Figure 5. Various host band discretisation schemes: (a) constant, (b) variable with a higher resolution at low energy, (c) variable with a higher resolution at intermediate energy, and (d) logarithmic.

constant discretisation for the same number of host band states, but the resolution is higher. In figure 3 we show the spectral density calculated using this scheme with a high resolution of $\Delta_\epsilon = 0.16 - 0.20\Delta_0$ inside each interval and a lower resolution of $\Delta_\epsilon = 0.71 - 0.76\Delta_0$ outside. The spectrum has been calculated with $\eta = 0.25\Delta_0$ then deconvolved (see next section). This spectrum is clearly sharper than the one obtained with a constant discretisation and, by comparison with related NRG and LMA results, it seems also more accurate. The improvement is due both to the lower broadening η and the deconvolution. Nevertheless, the variable discretisation scheme with varying broadening η is more accurate for low frequency and gives a much sharper Abrikosov-Suhl resonance.

As in NRG calculations [8] a logarithmic discretisation of the host band $\epsilon_k = (W/2)\Lambda^{-k}$ (with $\Lambda > 1$ and $k = 1, 2, \ldots, N/2$) is possible. Ground state DMRG calculations can easily been performed although the computational effort is significantly greater than with NRG. Calculating the spectral density with DDMRG is more problematic. The main problem is that we have not found any satisfactory method to broaden the spectrum. In NRG calculations [10] the spectrum is convolved with a function which vanishes for $\omega \to 0$ and broadens the spectrum on a logarithmic scale $\eta \propto \omega \sim \Delta\epsilon_k$. In DDMRG calculations we always get the spectrum convolved with a Lorentzian (14). To imitate the logarithmic broadening we have tried a "Lorentzian" broadening (14) with a variable $\eta = \eta(\omega') = \lambda\omega'$. Note that with the DDMRG method we can change η as a function of ω but not of ω' in (14). Fortunately, if $G_\sigma(\omega)$ is the impurity Green's function obtained with DDMRG for $\eta(\omega) = \lambda\omega$, the desired Green's function $\tilde{G}_\sigma(\omega)$ with $\eta(\omega') = \lambda\omega'$ can be obtained through

$$\tilde{G}_\sigma(\omega) = \frac{1 + i\lambda}{1 + \lambda^2}\, G_\sigma\left(\frac{\omega}{1 + \lambda^2}\right). \tag{19}$$

Note that the condition (17) implies $\lambda > 1 - \Lambda^{-1}$. We have tested this approach on the flat-band SIAM for various values of U. As expected, the high-energy spectrum is widely broadened and qualitatively similar to corresponding NRG results [10]. In the low-energy spectrum, however, this scheme clearly does not work because $D_\sigma(\omega)$ seems to diverge for $\omega \to 0$ or at least the Fermi level spectral density $D_\sigma(0)$ is much larger than the exact value $1/(\pi\Delta_0)$. We think that this failure is due to the broadening

with the Lorentzian function (14), which does not vanish for $\omega \to 0$ contrary to the function used in NRG calculations [10]. Therefore, a logarithmic discretisation does not seem to be useful for DDMRG calculations. It should be noted that with the Lanczos-DMRG [20] or the correction-vector DMRG [21] it should be possible to calculate the spectral density in the Lehmann representation (16) (i.e., without broadening) and to broaden it on a logarithmic scale as in NRG calculations. This approach could give better results for the low-energy spectrum than the DDMRG approach discussed here but has yet to be tested.

In summary, the host band discretisation determines the resolution of DDMRG calculations for the impurity spectral density. No single discretisation scheme is appropriate for all cases. Nevertheless, a combination of different schemes can be used for the various features of the same spectrum. Therefore, DDMRG allows one to calculate a spectral density with high resolution for all frequencies provided the host band discretisation and the broadening are adapted to the specific problem and its spectral features.

4. Deconvolution of DDMRG spectra

An approach for obtaining sharper spectra is the deconvolution of the DDMRG data. In theory, a deconvolution means solving (14) for $D(\omega)$ using the DDMRG data in the left-hand side. However, this is typically a ill-conditioned inversion problem [19] which generally cannot be solved numerically. Moreover, if it was possible to do this calculation exactly, one would obtain the discrete spectral density of the SIAM on a finite lattice of $N+1$ sites.

Nevertheless, the broadened spectral density of the SIAM on a infinite lattice ($N \to \infty$) is usually almost identical to the spectral density of the discretised SIAM ($N < \infty$). For instance, for $U = 0$ there is no visible difference in figure 2 between the DDMRG results for $N = 59$ and the exact result for $N \to \infty$. [A necessary condition for a large enough η is (17).] Therefore, one can make the approximation that DDMRG data for $D_\sigma^\eta(\omega)$ describe the broadened spectral density for $N \to \infty$ and solve (14) approximately under the condition that $D_\sigma(\omega)$ is the exact spectral density of the SIAM. For instance, one can require that $D_\sigma(\omega)$ is a continuous and relatively smooth function.

In practice, we calculate $D_\sigma(\omega)$ using the algorithm presented in [17] or using standard linear regularisation methods for the inverse problem [19]. Other possibilities include using Fourier transformations [18] or the Maximum Entropy Method as in QMC simulations [7]. In figure 2 one sees that the deconvolved DDMRG spectral density agrees perfectly with the exact result for $U = 0$. Similarly, a deconvolution gives excellent results for finite but weak coupling U. For $U = 2.5\pi\Delta_0$ the deconvolved spectral density in figure 3 shows sharper Abrikosov-Suhl resonance and Hubbard satellites than the original DDMRG data for $\eta = 0.25\Delta_0$ (not shown). However, the Friedel sum rule (8) at the Fermi level is far from being fulfilled (the relative error is

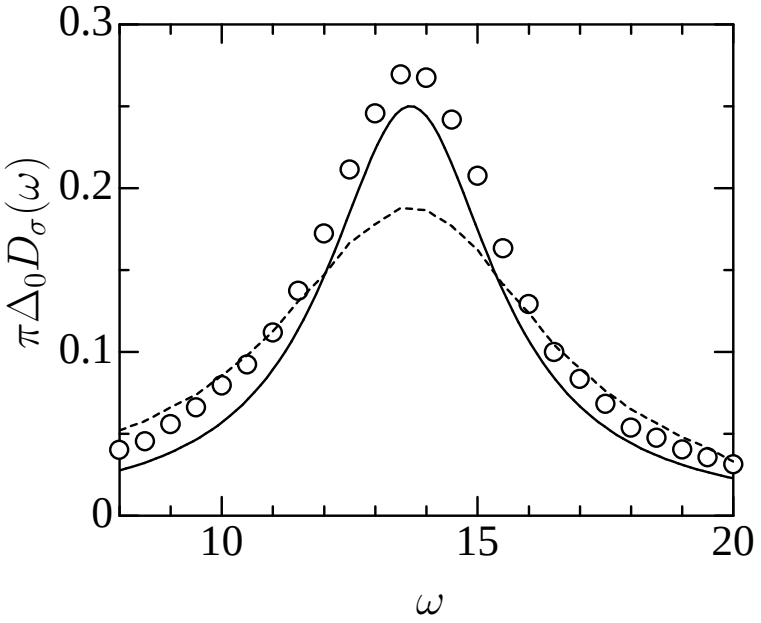

Figure 6. Upper Hubbard satellite for $U = 8\pi\Delta_0$. Calculated with DDMRG for $W = 40\Delta_0$ and a constant discretisation $\Delta\epsilon = 1.29\Delta_0$ and $\eta = \Delta_0$ (dashed line) then deconvolved (circles). The solid line shows the LMA result [5] for $U \gg \Delta_0$ (see text).

about 10 %), which indicates that the Fermi level resonance is still too broad despite the deconvolution. In general, we have found that the deconvolution works very well for the Hubbard satellites and other broad structures (broader than η) but bring only a partial improvement for sharp peaks.

Deconvolution methods become rapidly instable if a variable broadening η is used in (14). Therefore, we apply them to spectra calculated with a constant η only. Nevertheless, if the spectrum is made of well separated structures (as the Abrikosov-Suhl peak and the Hubbard satellites are for strong coupling $U \gg \Delta_0$), it is possible to deconvolve each structure separately. In that case we can use a different η for each structure. In figure 6 we show the upper Hubbard satellite calculated with DDMRG for $U = 8\pi\Delta_0$ then deconvolved. Our numerical result agrees remarkably well with the LMA prediction for this spectral structure in the strong coupling regime $U \gg \Delta_0$: a Lorentz distribution of width $2\Delta_0$ and total weight $\frac{1}{2}$ centered at $\omega_c = U/2$. Note that in figure 6 we have chosen $\omega_c = 13.7\Delta_0$ to fit our data rather than the value $\omega_c = U/2 = 4\pi\Delta_0 \approx 12.6\Delta_0$. This shift of $1.1\Delta_0$ is due to corrections to ω_c of the order of Δ_0/U [5] and the finite discretisation $\Delta\epsilon = 1.29\Delta_0$ used in our calculation. The deconvolved DDMRG spectral density appears to contain more spectral weight than the LMA result because we have used a rather narrow energy window $|\omega| < W/2 = 20\Delta_0$ in the DDMRG calculation and thus the spectral weight which normally lies in the high energy tail ($|\omega| > W/2$) of the Lorentz distribution has been shifted to low energy ($|\omega| < W/2$).

5. Conclusion

We have extended the DDMRG method [14] to the investigation of dynamic properties in quantum impurity problems. The method has been demonstrated on the flat-band symmetric SIAM. We have obtained accurate results for the impurity spectral density for all frequencies and coupling strengths. The main difficulty of this approach is the choice of an appropriate discretisation of the host band to resolve sharp spectral features such as the Abrikosov-Suhl resonance in the strong-coupling regime of the SIAM.

Our method can readily be used to study quantum lattice many-body systems in the framework of the DMFT. We have already applied this DDMRG-DMFT technique to the Hubbard model in infinite dimensions. For the metallic phase at weak coupling U our numerical results have a better resolution than those obtained with NRG and are in excellent agreement with weak-coupling perturbation theory [17]. In the Mott insulating phase DDMRG-DMFT calculations are relatively easy to perform because there is no sharp structure to resolve around $\omega = 0$. Thus we can obtain very accurate results for the Hubbard bands in the spectral density and determined the one-particle gap. Our numerical results agree remarkably well with strong-coupling perturbation theory [22]. We are currently investigating the intermediate-coupling regime, where the Mott metal-insulator transition occurs [23], using DDMRG-DMFT.

The DDMRG method presented here can be generalised and applied to a great variety of quantum impurity problems. First, although we have discussed only the symmetric flat-band SIAM, our method can readily be applied to an asymmetric SIAM [6] or more complicated hybridisation functions. Second, the method can be used for other Hamiltonians than the SIAM (for instance, the Kondo model) provided that the transformation to a one-dimensional lattice configuration with short-range interactions only is possible. Third, contrary to NRG our method can resolve sharp spectral structures at any frequency and thus could be very useful for studying the dynamics of systems with resonances at finite frequency, such as the Kondo model in magnetic field [24]. Fourth, DDMRG can be applied to models with other degrees of freedom than fermions. For instance, there are very efficient density-matrix renormalisation methods to treat bosons [25]. One can easily combine them with DDMRG to investigate a quantum degree of freedom coupled to a dissipative environment such as a phonon bath [26]. Finally, our method can be generalised to problems with more than one impurity or more than one host band. If the impurity sites are arranged in a one-dimensional lattice and the number of host bands do not exceed two, the computational effort is probably comparable to that required for the investigation of the SIAM presented here. Therefore, one should be able to investigate the dynamics of a two-channel Kondo problem or of quantum dots and wires coupled to (up to) two leads [3] without difficulty. If the impurity sites form other structures such as a two-dimensional cluster or the number of host bands is greater than two (which occurs for multi-channel Kondo problems or in the dynamical cluster approximation [27]), DDMRG calculations of dynamic properties are also possible but the computational effort could be

substantially greater. In summary, DDMRG provides a powerful and versatile approach for investigating the dynamics of quantum impurity problems.

Acknowledgments

We are deeply grateful to F Gebhard for suggesting the extension of DDMRG to quantum impurity problems and for many stimulating discussions. We also wish to thank T Pruschke, D Logan, T Costi and R Bulla for helpful discussions regarding the present work.

References

[1] Anderson P W 1961 *Phys. Rev.* **124** 41
[2] Hewson A C 1993 *The Kondo Problem to Heavy Fermions* (Cambridge: Cambridge University Press)
[3] Goldhaber-Gordon D et al 1998 *Nature* **391** 156
Cronenwett S M , Oosterkamp T H and Kouwenhoven L P 1998 *Science* **281** 540
[4] Brandt U and Mielsch C 1989 *Z. Phys.* B **75** 365
Brandt U and Mielsch C 1990 *Z. Phys.* B **79** 295
Jarrell M 1992 *Phys. Rev. Lett.* **69** 168
Georges A, Kotliar G, Krauth W and Rozenberg M 1996 *Rev. Mod. Phys.* **68** 13
[5] Logan D E, Eastwood M P and Tusch M A 1998 *J. Phys.: Condens. Matter* **10** 2673
[6] Glossop M T and Logan D E 2002 *J. Phys.: Condens. Matter* **14** 6737
[7] Silver R N, Gubernatis J E, Sivia D S and Jarrell M 1990 *Phys. Rev. Lett.* **65** 496
Gubernatis J E, Jarrell M, Silver R N and Sivia D S 1991 *Phys. Rev.* B **44** 6011
[8] Wilson K G 1975 *Rev. Mod. Phys.* **47** 773
[9] Frota H O and Oliveira L N 1986 *Phys. Rev.* B **33** 7871
Costi T A and Hewson A C 1992 *Phil. Mag.* B **65** 1165
Hofstetter W 2000 *Phys. Rev. Lett.* **85** 1508
[10] Bulla R, Hewson A C and Pruschke Th 1998 *J. Phys.: Condens. Matter* **10** 8365
[11] White S R 1992 *Phys. Rev. Lett.* **69** 2863
White S R 1993 *Phys. Rev.* B **48** 10345
[12] Peschel I, Wang X , Kaulke M and Hallberg K (Eds.) 1999 *Density-Matrix Renormalization* (Berlin: Springer-Verlag)
[13] Jeckelmann E, Gebhard F and Essler F H L 2000 *Phys. Rev. Lett.* **85** 3910
[14] Jeckelmann E 2002 *Phys. Rev.* B **66** 045114
[15] Sorensen E S and Affleck I 1995 *Phys. Rev.* B **51** 16115
Wang W, Qin S, Lu Z-Y, Yu L and Su Z 1996 *Phys. Rev.* B **53** 40
Wang X and Mallwitz S 1996 *Phys. Rev.* B **53** 492
Hallberg K and Egger R 1997 *Phys. Rev.* B **55** 8646
[16] Cazalilla M A and Marston J B 2002 *Phys. Rev. Lett.* **88** 256403
Luo H G, Xiang T and Wang X Q 2003 *Phys. Rev. Lett.* **91** 049701
Cazalilla M A and Marston J B 2003 *Phys. Rev. Lett.* **91** 049702
Berkovits R 2003 *Preprint* cond-mat/0306284
[17] Gebhard F, Jeckelmann E, Mahlert S, Nishimoto S and Noack R M 2003 *Preprint* cond-mat/0306438
[18] Raas C, Uhrig G S and Anders F B 2003 *Preprint* cond-mat/0309675
[19] Press W H, Teukolsky S A, Vetterling W T and Flannery B P 2002 *Numerical Recipes in C++* (Cambridge: Cambridge University Press)

[20] Hallberg K A, 1995 *Phys. Rev.* B **52** 9827
[21] Kühner T D and White S R 1999 *Phys. Rev.* B **60** 335
[22] Gebhard F, Jeckelmann E, Kalinowski E and Nishimoto S (in preparation)
[23] Gebhard F 1997 *The Mott Metal-Insulator Transition* (Berlin: Springer-Verlag)
[24] Rosch A, Costi T A, Paaske J and Wölfle P 2003 *Phys. Rev.* B **68** 014430
[25] Zhang C, Jeckelmann E and White S R 1998 *Phys. Rev. Lett.* **80** 2661
Zhang C, Jeckelmann E and White S R 1999 *Phys. Rev.* B **60** 14092
[26] Leggett A J et al. 1987 *Rev. Mod. Phys.* **59** 1
[27] Hettler M H, Tahvildar-Zadeh A N, Jarrell M, Pruschke T and Krishnamurthy H R 1998 *Phys. Rev.* B **58** 7475